Diagn Interv Radiol 2025; DOI: 10.4274/dir.2025.253371

HEAD AND NECK IMAGING

ORIGINAL ARTICLE

Magnetic resonance imaging findings in Ménière's disease: the impact of radiologist experience on hydrops imaging

Çağatay Cihan[1]
Uğur Toprak[1]
Emre Emekli[1,2]
Armağan İncesulu[3]
Hamit İpek[3]

[1]Eskişehir Osmangazi University Faculty of Medicine, Department of Radiology, Eskişehir, Türkiye

[2]Eskişehir Osmangazi University, Translational Medicine Application and Research Center, Eskişehir, Türkiye

[3]Eskişehir Osmangazi University Faculty of Medicine, Department of Ear Nose Throat, Eskişehir, Türkiye

Corresponding author: Emre Emekli

E-mail: emreemekli90@gmail.com

Received 08 April 2025; revision requested 08 May 2025 ; last revision received 07 July 2025; accepted 27 July 2025.

Epub: 18.08.2025

Publication date:

DOI: 10.4274/dir.2025.253371

PURPOSE

This study investigates the competence of a newly certified radiologist in reporting hydrops imaging and examines the role of magnetic resonance imaging (MRI) findings in diagnosing definite and probable Ménière's disease (MD).

METHODS

Sixty-four cases were retrospectively evaluated–blinded to clinical data–by a senior radiologist (O-1) and a newly certified radiologist (O-2) using 3D heavily T2-weighted and delayed contrast-enhanced three-dimensional fluid-attenuated inversion recovery sequences. The posterior fossa–posterior semicircular canal (P–P) distance, endolymphatic hydrops (EH), perilymphatic enhancement (PE), and the round window sign (RWS) were assessed.

RESULTS

Interobserver agreement was moderate for cochlear ($\kappa = 0.591$) and vestibular hydrops ($\kappa = 0.566$), good for PE ($\kappa = 0.663$), and excellent for the RWS ($\kappa = 0.817$). O-1 demonstrated good intraobserver agreement for the RWS ($\kappa = 0.787$) and excellent agreement for the other parameters. O-2 showed lower intraobserver agreement for cochlear hydrops, vestibular hydrops, and the RWS ($\kappa = 0.366$, $\kappa = 0.332$, and $\kappa = 0.398$, respectively). The P–P distance showed excellent interobserver [intraclass correlation coefficient (ICC) = 0.932] and intraobserver agreement (ICC = 0.978 for O-1; ICC = 0.886 for O-2). The P–P distance was significantly shorter in definite MD (dMD) than in probable MD (pMD) (1.23 ± 1.07 mm vs. 2.17 ± 1.79 mm, $P = 0.021$). The rate and grade of hydrops were higher in dMD ($P < 0.050$), whereas the RWS was more frequent in pMD. Hydrops and PE were more often observed on the symptomatic side ($P < 0.001$). Cochlear hydrops was identified in 14.3% and vestibular hydrops in 31.2% of asymptomatic sides.

CONCLUSION

The newly certified radiologist's intraobserver agreement for hydrops imaging was insufficient. In dMD, the retrolabyrinthine bone is thinner, hydrops is more frequent and advanced, and the RWS is less common. Approximately one in five patients with MD may have a perilymphatic fistula. Close monitoring of asymptomatic contralateral ears is essential.

CLINICAL SIGNIFICANCE

Accurate MRI evaluation of EH in MD strongly depends on the radiologist's expertise. This study highlights that newly certified radiologists may show lower reliability in assessing hydrops imaging, underscoring the need for targeted training programs.

KEYWORDS

Endolymphatic hydrops, magnetic resonance imaging , Meniere's disease, perilymphatic enhancement, perilymphatic fistula, round window sign

You may cite this article as: Cihan Ç, Toprak U, Emekli E, İncesulu A, İpek H. Magnetic resonance imaging findings in Ménière's disease: the impact of radiologist experience on hydrops imaging. *Diagn Interv Radiol*. 18 August 2025 DOI: 10.4274/dir.2025.253371 [Epub Ahead of Print].

Ménière's disease (MD) is a clinical syndrome characterized by spontaneous vertigo, fluctuating low-frequency sensorineural hearing loss, tinnitus, and aural fullness.[1] The 2015 diagnostic criteria classify MD into two categories: definite MD (dMD) and probable MD (pMD), based on the duration of vertigo attacks and the presence of low- to mid-frequency hearing loss.[1] However, in the early stages of the disease, key symptoms–such as vertigo, tinnitus, and hearing loss–may not occur simultaneously, complicating diagnosis.[2] The etiopathogenesis of MD is not fully understood, but it is associated with an excessive accumulation of endolymph, resulting in endolymphatic hydrops (EH). Due to overlapping clinical features, MD is often misdiagnosed as other conditions, such as vestibular migraine or vestibular schwannoma.[3-6]

Advancements in endolymphatic imaging have been made possible by 3 Tesla (3T) magnetic resonance imaging (MRI) systems. Nakashima et al.[7] conducted the first notable study in 2007, using intratympanic administration of a contrast agent. In 2010, the same group introduced intravenous contrast administration for endolymphatic imaging.[8] Imaging is typically performed approximately 4 hours after intravenous contrast injection, when the agent reaches peak concentration in the perilymph but does not enter the endolymph, allowing the endolymph to appear as negative contrast.[8]

Main points

- Magnetic resonance imaging (MRI) evaluation of endolymphatic hydrops (EH) in Ménière's disease (MD) is highly dependent on the radiologist's experience; newly certified radiologists may require additional training to achieve adequate diagnostic consistency.
- EH and perilymphatic enhancement on MRI are considerably more common and advanced on the symptomatic side in patients with definite MD (dMD) than in those with probable MD (pMD).
- Reduced retrolabyrinthine bone thickness (i.e., shorter posterior fossa–semicircular canal distance) measured by MRI may serve as a supportive imaging marker for dMD.
- The round window sign, suggestive of perilymphatic fistula, can mimic symptoms of MD–particularly in pMD cases–and was observed in approximately one-fifth of symptomatic patients.
- MRI may detect EH even on clinically asymptomatic sides, emphasizing the importance of bilateral evaluation and long-term follow-up.

Since Nakashima's pioneering studies, numerous investigations have focused on EH imaging. However, most rely on subjective visual assessments, raising concerns about reliability and reproducibility. A review of the literature shows few studies examining interobserver agreement and even fewer evaluating intraobserver agreement. These studies typically involve neuroradiologists or head and neck radiologists, often senior-level experts.[9-12] At our institution, hydrops imaging has been integrated into routine MRI scans for head and neck radiology since 2019. However, it is not yet standard practice in many countries, including ours, where it remains primarily a research topic. This study aims to evaluate the competence of a newly certified radiologist in hydrops imaging and to assess the diagnostic role of MRI findings in dMD and pMD.

Methods

Approval was obtained from the Eskişehir Osmangazi University Non-Interventional Clinical Research Ethics Committee (16.05.2023/58). As this was a retrospective study, the ethics committee waived the requirement for informed consent from the patients.

Magnetic resonance imaging protocol

MRI scans were performed using a 3T scanner (GE Discovery 750W, General Electric, Milwaukee, WI, USA) equipped with a 32-channel head coil. Fifty-four cases were scanned using the older version of the scanner, and 10 cases were scanned using the upgraded version. For the older version, 0.2 mmol/kg of a gadolinium-based contrast agent was administered intravenously, whereas 0.1 mmol/kg was used for the upgraded version.

The protocol for the delayed contrast-enhanced CUBE three-dimensional fluid-attenuated inversion recovery (3D-FLAIR) sequence on the older version was as follows: field of view (FOV) 260 mm, slice thickness 0.8 mm, repetition time (TR) 6,800 ms, echo time (TE) 115 ms, number of excitations (NEX) 1, inversion time (TI) 1,769 ms, matrix 320 × 288, bandwidth 42 Hz/pixel, echo train length (ETL) 200, voxel size 0.8 × 0.8 × 0.8 mm, and scan time 8 minutes. The protocol for the upgraded version was as follows: FOV 160 mm, slice thickness 0.4 mm, TR 8,500 ms, TE 168 ms, NEX 2, TI 2,185 ms, flip angle 142°, matrix 224 × 224, bandwidth 50 Hz/pixel, ETL 220, voxel size 0.7 × 0.7 × 0.8 mm, and scan time 6 minutes. The protocol for the heavily T2-weighted fast imaging employing steady-state acquisition (FIESTA) sequence was as follows: FOV 220 mm, slice thickness 0.8 mm, TR 5.4 ms, TE 2.1 ms, NEX 2, flip angle 55°, matrix 320 × 320, and scan time 5 minutes. This 3D-FLAIR sequence is T1-weighted and optimized for delayed post-contrast imaging to assess inner ear fluid compartments.

Patient selection

Between September 2019 and April 2023, MRI scans were performed. Patients were excluded from the study due to images of insufficient quality (motion artifacts, low contrast-to-noise ratio) or clinical diagnoses of vertigo or hearing loss (sensorineural and sudden sensorineural), leaving 86 patients with MD. Among these, 22 cases with a clinical diagnosis of bilateral MD were included in the radiological evaluation but excluded from statistical analysis to avoid bias related to disease laterality. Finally, 64 patients were included in the study (Figure 1).

The following patient characteristics were recorded: age, sex, symptomatic side (right or left), diagnostic classification (pMD or dMD), and history of intratympanic therapy (e.g., gentamicin). MRI evaluations included cochlear and vestibular hydrops grading, presence of perilymphatic enhancement (PE), the round window sign (RWS), and measurement of the posterior fossa–posterior semicircular canal (P–P) distance.

Interobserver and intraobserver agreement

The 64 patients included in the study were evaluated independently, twice each, by a radiologist with 20 years of experience in head and neck radiology and 5 years of experience in EH imaging (XX, O-1), and a newly certified radiologist with 5 years of general radiology experience (XX, O-2). During residency, O-2 completed three separate 3-month head and neck radiology rotations, during each of which they reviewed approximately 30 cases involving EH imaging. The observers were blinded to clinical findings, disease laterality, and whether symptoms were unilateral or bilateral. Each patient was evaluated twice by each observer, with a 2–4-week interval between the two evaluations. The assessments were performed using the GE Advantage Workstation VolumeShare 5 (General Electric, Milwaukee, WI, USA).

Image evaluation

Vestibular hydrops was evaluated on delayed contrast-enhanced 3D-FLAIR series using the Bernaerts classification (grade 0: normal-sized saccule and utricle; grade 1: the saccule is equal in size to or larger than the utricle; grade 2: confluence of saccule and utricle encompassing >50% of the vestibule; grade 3: total effacement of the perilymphatic space) (Figure 2). Cochlear hydrops (Figure 3 and 4) was evaluated using the Baráth classification (grade 1: mild dilatation of the non-enhancing cochlear duct; grade 2: uniform obstruction of the scala vestibuli by the severely distended cochlear duct).[13,14] Asymmetric PE (Figure 5)[15] and the presence of the RWS[16] were also investigated (Figure 6). In heavily T2-weighted images, the P–P distance (Figure 7) was measured as the distance from the posterior border of the vertical part of the posterior semicircular canal to the posterior cortex of the petrous bone, used as the reference.[10,17] In cases of discrepancy between the two evaluations, the radiologists jointly re-evaluated the imaging findings in a consensus session, during which both examiners reviewed the images together on the same workstation and reached an agreement through discussion. If disagreement persisted, the finding was recorded as "non-consensus" and excluded from the final agreement analysis.

Statistical analysis

Data were analyzed using (IBM, Armonk, NY, USA). A value of $P < 0.05$ was considered statistically significant. The Shapiro–Wilk test was used to assess the normality of continuous variables. McNemar's test was applied to compare findings between symptomatic and asymptomatic sides. The Wilcoxon test was used to compare P–P distances, whereas the Mann–Whitney U test compared the dMD and pMD groups. Chi-square and Fisher's exact tests were used for categorical comparisons. Interobserver and intraobserver agreement for P–P measurements was assessed using the intraclass correlation coefficient (ICC), and Cohen's kappa was used to analyze agreement for categorical variables.

Results

Interobserver and intraobserver agreement

The mean age of the 64 cases was 45.49 ± 10.81 years, with 35 women (54.7%) and 29 men (45.3%). A total of 43 cases (67.2%) were classified as pMD and 21 cases as dMD.

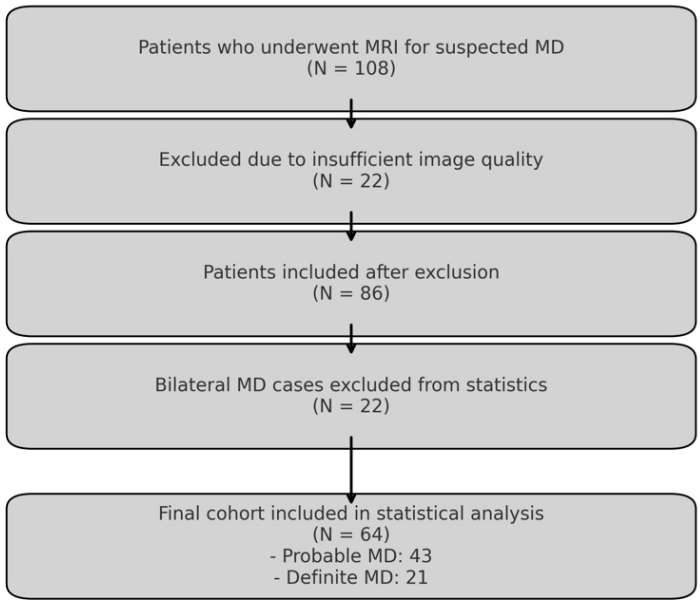

Figure 1. Patient selection flowchart. MRI, magnetic resonance imaging; MD, Ménière's disease.

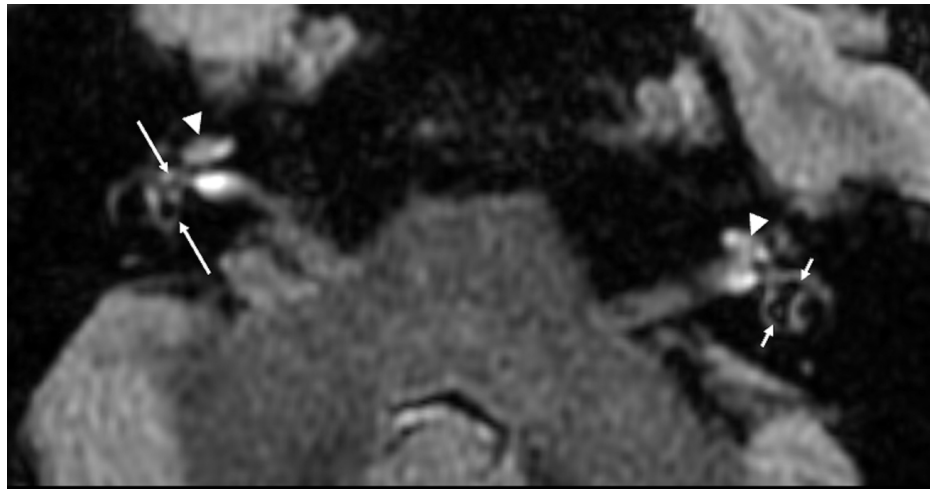

Figure 2. Axial delayed contrast-enhanced 3D-FLAIR images showing vestibular hydrops evaluation. On the right side, the saccule and utricle (long arrows) are normal in size and well separated (grade 0, Bernaerts classification).[19] On the left side, the saccule and utricle are confluent (short arrows), but the perilymphatic space remains partially visible, consistent with grade 2. Bilateral cochleae are marked with arrowheads. 3D-FLAIR, three-dimensional fluid-attenuated inversion recovery.

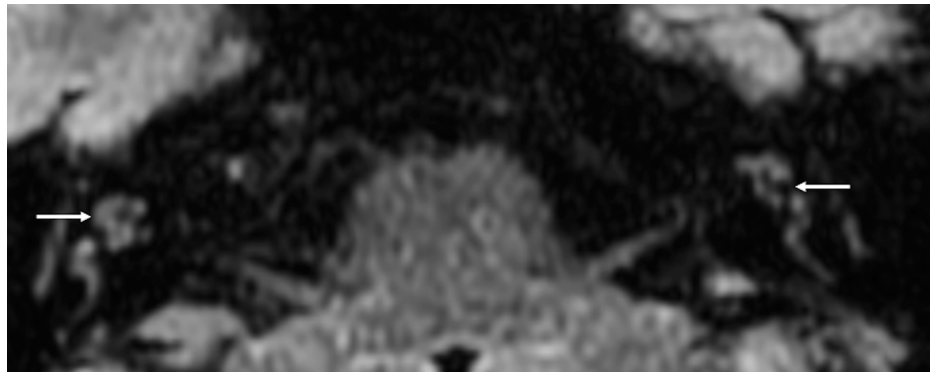

Figure 3. Axial delayed contrast-enhanced 3D-FLAIR image showing cochlear hydrops evaluation. On the left side, punctate non-enhancing areas within the cochlear duct (arrows) indicate grade 1 hydrops, according to the Baráth classification.[13] The right cochlea appears normal. 3D-FLAIR, three-dimensional fluid-attenuated inversion recovery.

In 36 patients (56.3%), the right side was symptomatic, whereas in 28 (43.8%), the left side was symptomatic.

Interobserver agreement was moderate for cochlear and vestibular hydrops, good for PE, and very good for the RWS (Table 1).

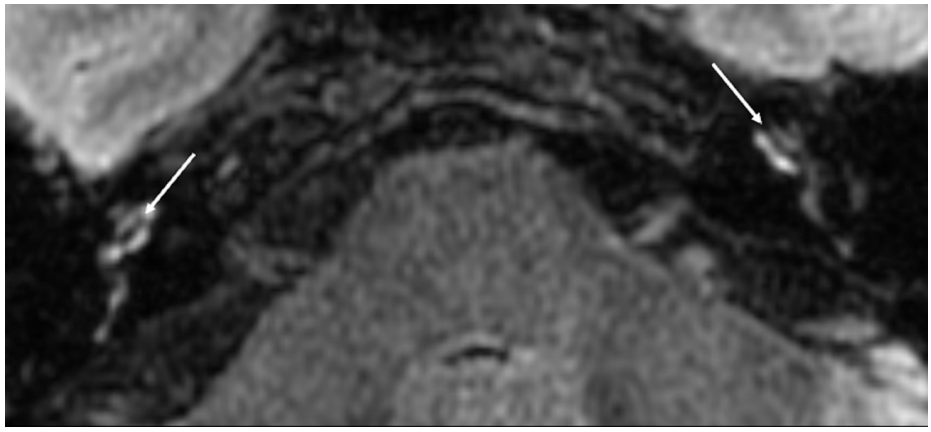

Figure 4. Axial delayed contrast-enhanced 3D-FLAIR image demonstrating bilateral grade 2 cochlear hydrops. Uniform dilation of the cochlear ducts (arrows) causes linear filling defects within the scala vestibuli, as defined by the Baráth classification.[13] 3D-FLAIR, three-dimensional fluid-attenuated inversion recovery.

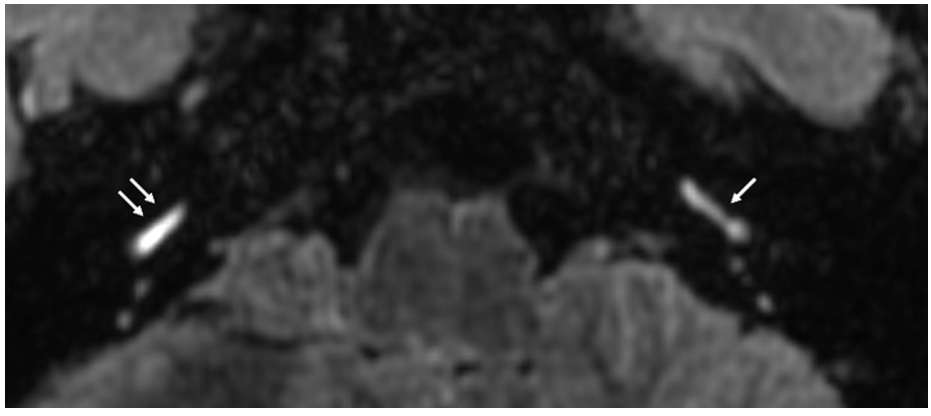

Figure 5. Axial delayed contrast-enhanced 3D-FLAIR image showing asymmetric perilymphatic enhancement. Increased contrast uptake is noted in the cochlear basal turn on the right side (arrows), compared with the left, consistent with asymmetric PE as described by Bernaerts et al.[19] 3D-FLAIR, three-dimensional fluid-attenuated inversion recovery; PE, perilymphatic enhancement.

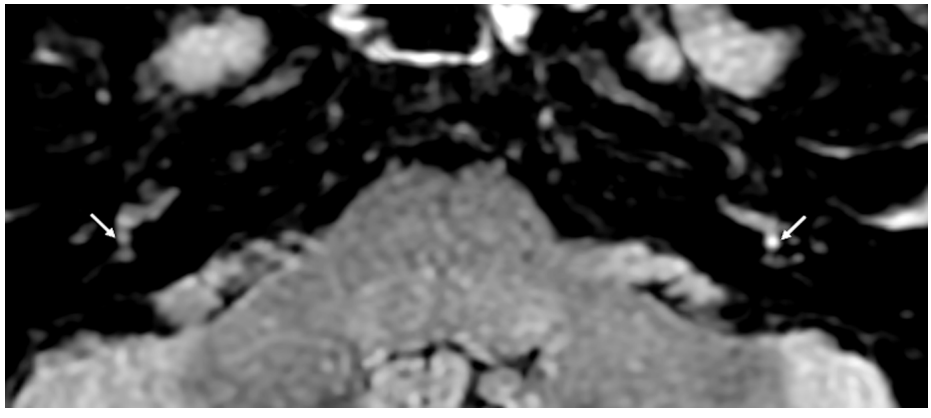

Figure 6. Axial delayed contrast-enhanced 3D-FLAIR image demonstrating high signal intensity in the left round window niche (arrow) in a patient with probable left-sided Ménière's disease, consistent with the round window sign suggestive of perilymphatic fistula, as described by Dubrulle et al.[16] The right round window niche appears normal (arrow). 3D-FLAIR, three-dimensional fluid-attenuated inversion recovery.

O-1's intraobserver agreement was good for the RWS and very good for the other criteria. O-2's intraobserver agreement was low (Table 2). For the P–P distance (n = 128), O-1 measured a mean of 1.87 ± 1.57 mm, whereas O-2 measured 1.67 ± 1.55 mm, with very good agreement [interobserver agreement: ICC = 0.932 (95% confidence interval; CI: 0.905–0.952), $P < 0.001$; intraobserver agreement: ICC = 0.978 for O-1 (95% CI: 0.960–0.989), ICC = 0.886 for O-2 (95% CI: 0.796–0.938), $P < 0.001$]. The P–P distance was shorter in cases of dMD than in pMD (1.23 ± 1.07 mm vs. 2.17 ± 1.79 mm, $P = 0.021$), but the difference between the normal sides was not significant (1.36 ± 1.14 mm vs. 2.13 ± 1.61 mm, $P = 0.056$).

Radiologic evaluation

On the asymptomatic side, grade 1 cochlear hydrops was observed in 5/64 cases (7.8%) and grade 2 in 4/64 cases (6.3%). Vestibular hydrops was grade 1 in 7/64 cases (10.9%) and grade 2 in 13/64 cases (20.3%). No grade 3 vestibular hydrops was observed on the asymptomatic side. PE was observed in 2/64 cases (3.1%), and the RWS was seen in 8/64 cases (12.5%), equal to the symptomatic side.

The comparison of radiological findings between the symptomatic and asymptomatic sides is presented in Table 3. On the symptomatic side, cochlear hydrops, vestibular hydrops, and PE were significantly more frequent than on the asymptomatic side ($P < 0.001$). The presence of the RWS was similar on both sides ($P > 0.05$).

On the symptomatic side, in cases of dMD, the rate of grade 2 cochlear hydrops (7/21 vs. 3/43; $P = 0.032$) and grade 3 vestibular hydrops (10/21 vs. 3/43; $P < 0.001$) was higher than in pMD. The rates of the RWS (3/21 vs. 5/43; $P = 1$) and PE (9/21 vs. 12/43; $P = 0.232$) were similar between the groups.

In 15 symptomatic ears (13 pMD, 2 dMD), neither EH nor PE was observed. In 3 of these 15 cases, the RWS was present (2 pMD, 1 dMD). In total, the RWS was detected in 8 symptomatic ears (5 pMD, 3 dMD) and on the asymptomatic side, including 6 cases of bilateral MD. On the symptomatic side, PE accompanied the RWS in 3 out of 8 ears. Among the 8 symptomatic ears with the RWS, EH (3 cochlear, 5 vestibular) was observed in 3 cases, along with PE. On the asymptomatic side, EH was observed in 4 cases (1 cochlear, 3 vestibular), but no PE was detected. No soft tissue

or effusion indicating hyperintensity in the area corresponding to the RWS was observed on the heavily T2-weighted sequences.

Bilateral RWS was observed in one patient with dMD who had undergone intratympanic gentamicin therapy, whereas bilateral grade 1 vestibular hydrops was noted in another patient. None of the other patients included in the study had a history of intratympanic therapy.

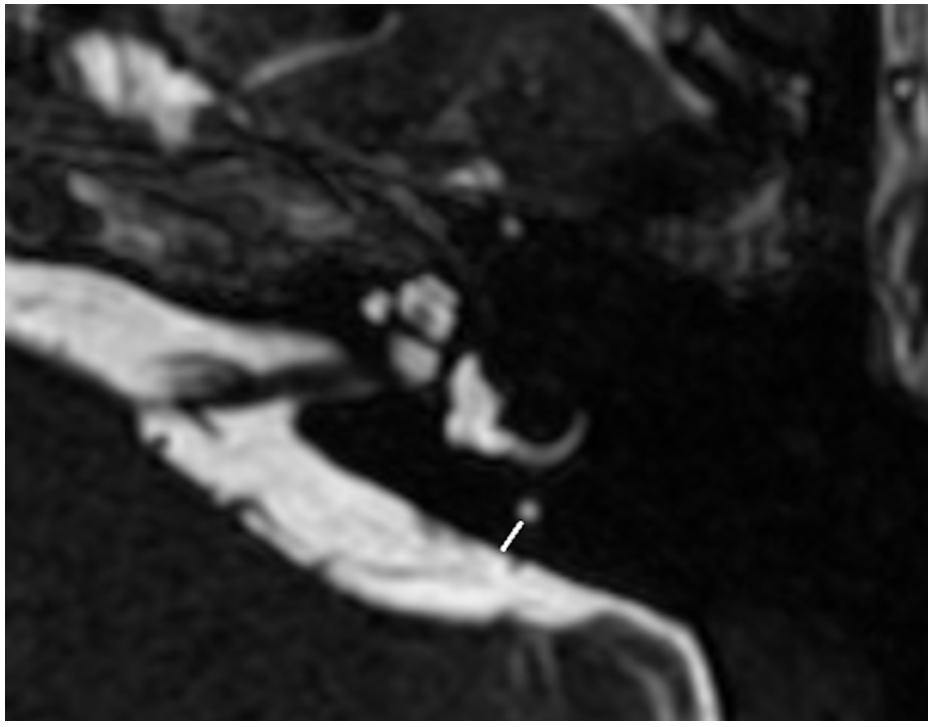

Figure 7. Coronal heavily T2-weighted FIESTA image showing measurement of the posterior fossa–posterior semicircular canal distance. The line indicates the shortest distance between the posterior border of the vertical limb of the posterior semicircular canal and the posterior cortical surface of the petrous temporal bone, used as an indicator of retrolabyrinthine bone thickness, as described by Lei et al.[10] FIESTA, fast imaging employing steady-state acquisition.

Discussion

In our study, interobserver agreement was moderate for cochlear and vestibular hydrops and good for visual PE evaluation. The 2022 study by Bernaerts et al.[18] reported similar agreement rates among senior neuroradiologists for cochlear and vestibular hydrops, as well as for visual PE evaluation using turbo spin-echo (TSE) FLAIR sequences. However, agreement was considerably higher in their study when using SPACE FLAIR sequences for hydrops and PE assessment. Their 2019 study also reported higher interobserver agreement, reaching a good level.[19] In the 2022 study by Deng et al.[20], interobserver agreement for vestibular hydrops using TSE FLAIR was good, and for cochlear hydrops, it was very good. That study also demonstrated even higher agreement when using real inversion recovery (IR) sequences. As previously noted, IR sequences developed after TSE FLAIR improved geometrical resolution, resulting in higher agreement rates. Studies using these sequences have reported near-perfect agreement among senior researchers.[9-12]

Table 1. Interobserver agreement for categorical data

Observer 1\observer 2		None	Present/grade 1	Grade 2	Grade 3	Kappa	*P*
Vestibular hydrops	**None**	53	5	6	0	0.566	<0.001
	Grade 1	8	7	4	0		
	Grade 2	4	4	23	1		
	Grade 3	0	0	4	9		
Cochlear hydrops	**None**	83	7	5		0.591	<0.001
	Grade 1	7	11	1			
	Grade 2	0	3	11			
Perilymphatic enhancement	**None**	95	10			0.663	<0.001
	Present/grade 1	4	19				
Round window sign	**None**	110	2			0.817	<0.001
	Present/grade 1	3	13				

Table 2. Intraobserver agreement for categorical data

	Observer-1		Observer-2	
	Kappa	*P*	Kappa	*P*
Cochlear hydrops	851	<0.001	366	0.001
Vestibular hydrops	964	<0.001	332	<0.001
Perilymphatic enhancement	908	<0.001	590	<0.001
Round window sign	787	<0.001	398	0.002

Table 3. Comparison of magnetic resonance imaging findings between symptomatic and asymptomatic sides of the cases

Symptomatic side/asymptomatic side		None	Present	*p*
Cochlear hydrops	**None**	38 (59.4)	2 (3.0)	<0.001
	Present	17 (26.6)	7 (11.0)	
Vestibular hydrops	**None**	18 (28.1)	2 (3.0)	<0.001
	Present	26 (40.7)	18 (28.2)	
Perilymphatic enhancement	**None**	41 (64.2)	2 (3.0)	<0.001
	Present	21 (32.8)	0	
Round window sign	**None**	54 (84.6)	2 (3.0)	0.001
	Present	2 (3.0)	6 (9.4)	

Good agreement was achieved for the RWS, which had not been evaluated for interobserver agreement in previous studies. The acceptable level of agreement in identifying the RWS–a clinically important abnormality that can mimic MD and is treatable through surgery–is noteworthy. Since the measurement site is defined and quantitative, P–P measurements also demonstrated very good agreement.

The experienced radiologist's intraobserver agreement for EH and PE was higher in our study than in the study by Bernaerts et al.[18], which used the TSE FLAIR sequence, achieving very good agreement. Agreement for the RWS was good. In contrast, the general radiologist's intraobserver agreement was low for EH and the RWS and moderate for PE, indicating that MR evaluation of hydrops in general radiology practice–without more quantitative criteria or higher-resolution sequences–remains a challenge.

Generally, kappa values above 0.60 are considered sufficient, but ideally, a value above 0.70 is targeted, as this indicates "good agreement" in medical studies.[21-23] When good agreement is considered the acceptable threshold, the values obtained in this study are insufficient. The low intraobserver agreement for hydrops imaging by the newly certified radiologist (O-2) suggests that limited experience in diagnosing MD may lead to clinically important discrepancies. Since hydrops imaging is not yet routinely integrated into clinical practice, the need for specialized training to ensure accurate application of this technique becomes apparent. In this context, structured training or mentorship programs led by experienced radiologists in centers that perform hydrops assessments, along with technological solutions to enhance reliability–such as automatic classification algorithms or artificial intelligence (AI)-supported analysis systems–should be developed. These findings highlight the importance of targeted education and structured training for radiologists, particularly in interpreting EH imaging. The relatively low intraobserver agreement observed in the newly certified radiologist underscores a gap that could be addressed through formalized curricula. Recent national-level data also indicate that radiology residents, despite having high awareness of technological terms such as AI and advanced imaging methods, often lack formal training and hands-on experience.[24] International standards–such as the European Training Curriculum developed by the European Society of Radiology and the curriculum of the European Society of Head and Neck Radiology–advocate for subspecialty-level training in head and neck imaging. Incorporating EH imaging into such curricula, particularly with standardized assessment protocols and hands-on case review, could enhance diagnostic reproducibility and clinical confidence among radiologists at various stages of training. This approach would support the routine use of hydrops imaging by improving diagnostic accuracy and reliability.

In this study, cochlear and vestibular hydrops and PE were considerably more frequent on the symptomatic side than on the asymptomatic side. Bernaerts et al.[19] demonstrated that cochlear PE and vestibular EH are the two most distinguishing features for differentiating symptomatic ears from asymptomatic ones. This finding is confirmed by the study of Van Steekelenburg et al.[25] In cases of dMD, the rate of grade 2 cochlear hydrops was higher on the affected side than in cases of pMD. Similarly, the rate of grade 3 vestibular hydrops was higher in dMD than in pMD, consistent with previous studies.[9]

EH does not always cause MD symptoms, and not all patients diagnosed with MD have EH.[16] In this study, 15 of 64 (23.4%) symptomatic ears (13 pMD, 2 dMD) had neither EH nor PE. Previous studies also failed to detect EH by MRI in 10%–33% of patients with MD.[13,26,27] Of these cases, 3 of 15 (20%) had the RWS (2 pMD, 1 dMD). On the asymptomatic side, 14.3% had cochlear hydrops, and 31.2% had saccular hydrops. These rates are higher than those reported in previous studies, which showed a maximum of 6.7% and 8.3%, respectively.[9,28] Differences in grading systems, such as those used by Ito et al.[28], may explain this discrepancy. The relatively high rate of hydrops detected on asymptomatic sides in our study, compared with previous reports, may also be explained by differences in patient selection criteria, sample composition, or hydrops grading systems. Nevertheless, it is notable that no cases of grade 3 hydrops were identified on the asymptomatic side in our cohort.

Perilymphatic fistula (PLF) can mimic MD symptoms, and it is extremely difficult to differentiate it from MD clinically, especially in the case of pMD.[29] The RWS has been previously described as a localized high signal covering the round window on 3D-FLAIR, indicating PLF.[16,30] PLF's clinical symptoms are highly variable and non-specific. Motion intolerance, fluctuating hearing loss, dizziness with or without true vertigo, tinnitus, and aural fullness are the most common symptoms. Symptoms can worsen with changes in pressure (such as during air travel, mountain climbing, rapid elevator rides, bending, lifting heavy objects, coughing, or sneezing) due to increased cerebrospinal fluid pressure. Although initial symptoms may be either entirely auditory or vestibular, many patients develop both types of symptoms over time.[16] Unlike most other causes of sensorineural hearing loss and dizziness, PLF can be corrected surgically by repairing the fistula.[31,32] Based on the results of this study, the RWS, potentially representing PLF, was recorded in 8/64 (12.5%) cases, mostly in pMD cases (11.6%, 5/43). The majority of RWS findings in the study by Dubrulle et al.[16] were also seen in patients with pMD.

In this study, the RWS was also observed in 8 asymptomatic sides (6 bilateral MD cases). However, EH accompanied the RWS in 4 asymptomatic sides (3 vestibular), with no PE in any of them. In the study by Attyé et al.[30], 2/30 healthy volunteers also had the RWS.[29] Our study lacked a healthy volunteer group, so asymptomatic sides were used as controls, and EH was observed in 34% of asymptomatic sides, mostly low-grade. No soft tissue or hyperintensity suggesting inflammation in the round window niche was observed on the FIESTA sequence corresponding to the RWS in any case.

Unilateral defunction therapy is increasingly being used in patients requiring deep vestibular deafferentation to effectively control vertigo symptoms.[33] In our study, two patients with dMD had a history of intratympanic gentamicin application. One patient had bilateral RWS (on both the symptomatic side where the application was performed and the asymptomatic side), whereas the other had bilateral grade 1 vestibular hydrops. Attyé et al.[30] reported a correlation between the presence of PLF and a history of intratympanic gentamicin application. However, in our case, the RWS was observed on the asymptomatic side where no injection had been administered. Additionally, their study reported that three patients with vestibular hydrops also had PLF, and all had a history of intratympanic gentamicin application. In our second case, a similar vestibular hydrops was observed, but it was also present on the asymptomatic side. Therefore, contrary to the findings of their study, in both of our cases, the RWS and hydrops were detected on the asymptomatic side. Further studies with larger patient and control groups are needed on this topic.

In MD, aside from EH, retrolabyrinthine bone thickness has also been investigated. One study found that the distance between the vertical portion of the posterior semicircular canal and the posterior fossa was shorter in patients with unilateral MD than in patients with ipsilateral delayed EH and healthy controls.[10] In our study, in contrast to the study by Lei et al.[10], hydrops imaging was performed alongside heavily T2-weighted anatomical sequences, and dMD and pMD were compared rather than delayed EH cases and healthy controls. The P–P distance was found to be considerably shorter in dMD than in pMD. Recent literature has shown that this distance is associated with the hypoplastic MD endotype.[34,35] This finding supports the role of the hypoplastic endolymphatic sac in the pathogenesis of MD. Hypoplastic retrolabyrinthine bone thickness is proposed as a radiological marker with the potential to specifically identify the hypoplastic endotype of MD. Given the high interobserver agreement rates, incorporating retrolabyrinthine bone thickness measurement into the routine radiological evaluation for diagnosing the hypoplastic endotype of MD may enhance diagnostic accuracy.

There are several limitations to this study. First, the number of patients with dMD was relatively small. Second, the use of different imaging parameters may have complicated the evaluation. Third, the absence of sequences other than 3D-FLAIR may have limited interobserver agreement for hydrops evaluation. However, acquiring additional sequences involves higher costs, and such sequences are not yet widely available. Fourth, this study used clinically normal contralateral ears as the control group, and these control ears showed cochlear hydrops in 9 cases and vestibular hydrops in 20 cases (a total of 22 cases, 34.3%). Given that the 2015 criteria of the Bárány Society[1] still regard clinical, auditory, and vestibular function tests as the gold standard for diagnosing MD–and that MD is clinically limited to 1 ear in most cases–we used normal-appearing contralateral ears as controls. In addition, we employed two different classification systems: the Baráth classification for cochlear hydrops and the Bernaerts classification for vestibular hydrops. Although this approach is consistent with the existing literature and allows for structure-specific grading, it may reduce interpretive consistency and complicate reproducibility.

Lastly, the specificity of the RWS on delayed post-contrast 3D-FLAIR imaging remains a concern. Although the RWS has been proposed as a radiologic indicator of PLF, similar signal enhancement may occur in other inner ear conditions due to alterations in the blood–labyrinth barrier, particularly near the basal turn of the cochlea. As surgical confirmation was not available in our cases, definitive correlation with PLF could not be established. Therefore, the RWS findings should be interpreted with caution and always in the context of clinical data.

In conclusion, the agreement coefficients of the newly certified radiologist trained in hydrops imaging using current criteria were insufficient for evaluating hydrops MRI scans. When considered alongside existing literature, the findings suggest that higher-resolution sequences and more quantitative diagnostic criteria may improve evaluation accuracy. In dMD, the retrolabyrinthine bone is thinner, hydrops is more frequent and advanced, and the RWS is less common. One in five patients clinically diagnosed with MD may have PLF. Asymptomatic contralateral ears, which may also be hydropic, should be closely monitored.

Footnotes

Conflict of interest disclosure

The authors declared no conflicts of interest.

References

1. Lopez-Escamez JA, Carey J, Chung WH et al. Diagnostic criteria for Menière's disease. *J Vestib Res.* 2015;25(1):1-7. [CrossRef]
2. Nakashima T, Pyykkö I, Arroll MA, et al. Meniere's disease. *Nature Reviews Disease Primers*. 2016;2:1-18. [CrossRef]
3. Pyykkö I, Manchaiah V, Färkkilä M, Kentala E, Zou J. Association between Ménière's disease and vestibular migraine. *Auris Nasus Larynx.* 2019;46(5):724-733. [CrossRef]
4. Neff BA, Staab JP, Eggers SD, et al. Auditory and vestibular symptoms and chronic subjective dizziness in patients with Ménière's disease, vestibular migraine, and Ménière's disease with concomitant vestibular migraine. *Otol Neurotol.* 2012;33(7):1235-1244. [CrossRef]
5. Brantberg K, Baloh RW. Similarity of vertigo attacks due to Meniere's disease and benign recurrent vertigo, both with and without migraine. *Acta Otolaryngol.* 2011;131(7):722-727. [CrossRef]
6. Kentala E, Pyykkö I. Vestibular schwannoma mimicking Ménière's disease. *Acta Otolaryngol Suppl*. 2000;120:17-19. [CrossRef]
7. Nakashima T, Naganawa S, Sugiura M, et al. Visualization of endolymphatic hydrops in patients with Meniere's disease. *Laryngoscope.* 2007;117:415-420. [CrossRef]
8. Nakashima T, Naganawa S, Teranishi M, et al. Endolymphatic hydrops revealed by intravenous gadolinium injection in patients with Ménière's disease. *Acta Otolaryngol.* 2010; 130(3):338-343. [CrossRef]
9. Li J, Wang L, Hu N, et al. Improving diagnostic accuracy for probable and definite Ménière's disease using magnetic resonance imaging. *Neuroradiology.* 2023;65:1371-1379. [CrossRef]
10. Lei P, Leng Y, Li J, Zhou R, Liu B. Anatomical variation of inner ear may be a predisposing factor for unilateral Ménière's disease rather than for ipsilateral delayed endolymphatic hydrops. *Eur Radiol.* 2022;32:3553-3564. [CrossRef]
11. Sousa R, Lobo M, Cadilha H, Eça T, Campos J, Luis L. Is there progression of endolymphatic hydrops in Ménière's disease? Longitudinal magnetic resonance study. *Eur Arch Otorhinolaryngol.* 2023;280(5):2225-2235. [CrossRef]
12. Li J, Jin X, Kong X, et al. Correlation of endolymphatic hydrops and perilymphatic enhancement with the clinical features of Ménière's disease. *Eur Radiol.* 2024;34;6036-6046. [CrossRef]
13. Baráth K, Schuknecht B, Monge Naldi A, Schrepfer T, Bockisch CJ, Hegemann SCA. Detection and grading of endolymphatic hydrops in Menière disease using MR imaging. *AJNR Am J Neuroradiol.* 2014;35(7):1387-1392. [CrossRef]

14. Nakashima T, Naganawa S, Pyykkö I, et al. Grading of endolymphatic hydrops using magnetic resonance imaging. *Acta Otolaryngol Suppl.* 2009;560:5-8. [CrossRef]
15. Bernaerts A, De Foer B. Imaging of Ménière disease. *Neuroimaging Clin N Am.* 2019;29(1):19-28. [CrossRef]
16. Dubrulle F, Chaton V, Risoud M, Farah H, Charley Q, Vincent C. The round window sign: a sensitive sign to detect perilymphatic fistulae on delayed postcontrast 3D-FLAIR sequence. *Eur Radiol.* 2020;30(11):6303-6310. [CrossRef]
17. Osman S, Hautefort C, Attyé A, Vaussy A, Houdart E, Eliezer M. Increased signal intensity with delayed post contrast 3D-FLAIR MRI sequence using constant flip angle and long repetition time for inner ear evaluation. *Diagn Interv Imaging.* 2022;103(4):225-229. [CrossRef]
18. Bernaerts A, Janssen N, Wuyts FL, et al. Comparison between 3D SPACE FLAIR and 3D TSE FLAIR in Menière's disease. *Neuroradiology.* 2022;64:1011-1020. [CrossRef]
19. Bernaerts A, Vanspauwen R, Blaivie C, et al. The value of four stage vestibular hydrops grading and asymmetric perilymphatic enhancement in the diagnosis of Menière's disease on MRI. *Neuroradiology.* 2019;61:421-429. [CrossRef]
20. Deng W, Lin X, Su Y, Cai Y, Zhong J, Ou Y. Comparison between 3D-FLAIR and 3D-real IR MRI sequences with visual classification method in the imaging of endolymphatic hydrops in Meniere's disease. *Am J Otolaryngol.* 2022;43(6):103557. [CrossRef]
21. Sun S. Meta-analysis of Cohen's kappa. *Health Serv Outcomes Res Methodol.* 2011;11:145-163. [CrossRef]
22. Li M, Gao Q, Yu T. Kappa statistic considerations in evaluating inter-rater reliability between two raters: which, when and context matters. *BMC Cancer.* 2023;23(1):799. [CrossRef]
23. Sim J, Wright CC. The Kappa statistic in reliability studies: use, interpretation, and sample size requirements. *Phys Ther.* 2005;85(3):257-268. [CrossRef]
24. Emekli E, Coşkun O, Budakoğlu İİ. The role of the role of artificial intelligence in radiology residency training: a national survey study. *Eur J Ther.* 2024;30(6):844-849 [CrossRef]
25. Van Steekelenburg JM, Van Weijnen A, De Pont LMH, et al. Value of endolymphatic hydrops and perilymph signal intensity in suspected Ménière disease. *AJNR Am J Neuroradiol.* 2020;41(3):529-534. [CrossRef]
26. Kim WB, Pope AR, Sepahdari MN, et al. Blood-labyrinth barrier permeability in Menière disease and idiopathic sudden sensorineural hearing loss: findings on delayed postcontrast 3D-FLAIR MRI. *AJNR Am J Neuroradiol.* 2016;37(10):1903-1908. [CrossRef]
27. Pyykkö I, Nakashima T, Yoshida T, Zou J, Naganawa S. Ménière's disease: a reappraisal supported by a variable latency of symptoms and the MRI visualisation of endolymphatic hydrops. *BMJ Open.* 2013;3(2):001555. [CrossRef]
28. Ito T, Kitahara T, Inui H, et al. Endolymphatic space size in patients with Meniere's disease and healthy controls. *Acta Otolaryngol.* 2016;136:879-882. [CrossRef]
29. Lopez-Escamez JA, Carey J, Chung WH, et al. Diagnostic criteria for Menière's disease. *J Vestib Res.* 2015;25(1):1-7. [CrossRef]
30. Attyé A, Eliezer M, Galloux A, et al. Endolymphatic hydrops imaging: differential diagnosis in patients with Meniere disease symptoms. *Diagn Interv Imaging.* 2017;98(10):699-706. [CrossRef]
31. Foster PK. Autologous intratympanic blood patch for presumed perilymphatic fistulas. *J Laryngol Otol.* 2016;130(12):1158-1161. [CrossRef]
32. Deveze A, Matsuda H, Elziere M, Ikezono T. Diagnosis and treatment of perilymphatic fistula. *Adv Otorhinolaryngol.* 2018;81:133-145. [CrossRef]
33. Junet P, Karkas A, Dumas G, Quesada JL, Schmerber S. Vestibular results after intratympanic gentamicin therapy in disabling Menière's disease. *Eur Arch Otorhinolaryngol.* 2016;273(10):3011-3018. [CrossRef]
34. Bächinger D, Filidoro N, Naville M, et al. Radiological feature heterogeneity supports etiological diversity among patient groups in Meniere's disease. *Sci Rep*. 2023;13(1):10303. [CrossRef]
35. Juliano AF, Lin KY, Shekhrajka N, Shin D, Rauch SD, Eckhard AH. Retrolabyrinthine bone thickness as a radiologic marker for the hypoplastic endotype in Menière disease. *AJNR Am J Neuroradiol*. 2024;45(9):1363-1369. [CrossRef]